JTTEE5 17:908–914
DOI: 10.1007/s11666-008-9274-1
1059-9630/$19.00 © ASM International

Predicting Quenching and Cooling Stresses within HVOF Deposits

J. Stokes and L. Looney

(Submitted June 13, 2008; in revised form September 22, 2008)

Due to the nature of the HVOF and other thermal spray processes, residual stress build up in thick deposits is a significant and limiting problem since it impedes the coating behavior in service. The residual stress-state that evolves in a deposit is largely dependent on the thermal conditions to which the substrate/coating system has been subjected, and is a combination of quenching stresses, peening stresses that develop in some cases in HVOF, both of which arise during deposition, and cooling stresses, postdeposition. It follows that precise control of these phenomena is essential, if a thick deposit or one with low levels of residual stress are to be thermally sprayed. This paper applies looks at analytical and finite element techniques used to predict quenching and cooling stresses within tungsten carbide-cobalt thermally sprayed deposits. The analysis investigates and predicts the quenching and cooling stresses using improved analytical and finite element analysis techniques by validating the models with experimental results such as X-ray diffraction and the hole drilling method. The result of this paper is a thermo-mechanical equation for quenching stress which includes the effects of misfit strain, the Poisson's effect, variation of coating and substrate thicknesses, thermal expansion, and process temperature effects.

Keywords cooling stresses, HVOF thermal spraying, quenching stresses, residual stress

1. Introduction

The HVOF thermal spray system is most often used for deposition wear resistant coatings, WC-Co type coatings are typical of such an application. Challenges do exist in using HVOF thermal spraying for the purpose of depositing thicknesses greater than 1 mm without causing cracks to form or delamination of the deposit. It is important to be able to predict the level of residual stress within a thermal spray deposit in order to control and reduce its build-up by adjusting the operating spray parameters. It has been shown in previous research (Ref 1, 2) that increasing the thickness of the deposit increases the residual stress promoting fracture or failure of such coatings. Thermal spraying techniques not only produce thin deposits, but have also been shown to achieve thicknesses of several millimeters with the use of forced cooling (Ref 1-5). Due to the recent advances in thermal spra ying technology, considerable research emphasis has been placed on the development of models capable of predicting what happens at various stages during the process. In order to gain a deeper knowledge of the residual stress, one needs to rely on simple models or equations to provide us with the necessary residual stress predictions required to reduce residual stresses.

Nomenclature

σ_{RS}	residual stress (MPa)
σ_q	quenching stress (MPa)
σ_c	cooling stress (MPa)
$\sigma_{coating}$	coating stress (MPa)
$\sigma_{Substrate}$	substrate stress (MPa)
α_c	coefficient of thermal expansion of the coating (/K)
α_s	coefficient of thermal expansion of the substrate (/K)
T_m	lamella melting temperature (K)
T_s	substrate temperature (K)
T_R	room temperature (K)
E_c	coating Young's modulus (GPa)
E_s	substrate Young's modulus (GPa)
ν_c	coatings Poisson's ratio
ν_s	substrate Poisson's ratio
t_c	coating thickness (m)
t_s	substrate thickness (m)
κ	coatings curvature (m)
δ	shift of neutral axis (m)
$\Delta\varepsilon$	misfit strain

This article is an invited paper selected from presentations at the 2008 International Thermal Spray Conference and has been expanded from the original presentation. It is simultaneously published in *Thermal Spray Crossing Borders, Proceedings of the 2008 International Thermal Spray Conference*, Maastricht, The Netherlands, June 2-4, 2008, Basil R. Marple, Margaret M. Hyland, Yuk-Chiu Lau, Chang-Jiu Li, Rogerio S. Lima, and Ghislain Montavon, Ed., ASM International, Materials Park, OH, 2008.

J. Stokes and **L. Looney**, Materials Processing Research Centre & National Centre for Plasma Science and Technology, Dublin City University, Glasnevin, Dublin 9, Ireland. Contact e-mail: joseph.t.stokes@dcu.ie.

Residual stress build up within the coating structure has been modeled by several authors (Ref 6-14). All of these models treat the residual stresses as differential thermal contraction only that is due to the mismatch between the deposit and the substrate. However, residual stresses arise from two main sources, initially due to 'intrinsic' or quenching stresses developed during deposition and then due to cooling stresses (due to the mismatch of the materials). As quenching stresses were ignored, therefore differences between the experimental and finite element analysis (FEA) results were expected. The difference between the deposit properties (such as Young's apparent modulus and Poisson's ratio) used in the simulation, often differ from the actual properties of the material, thus adding to the differences found between results (Ref 8). Stokes (Ref 4) produced both a generated moment and thermal models, which were combined and compare this with both analytical and experiment results. Finite element analysis modeling is a useful tool, used to predict an outcome of a particular engineering situation, however it can be time consuming to implement, hence the ideal situation is to have analytical equations to predict the residual stresses and individual quenching and cooling stresses which can predict the stresses quickly and directly. However, it can be difficult to find equations to predict quenching stresses for both thick and thin deposits, as certain derivations are dependant on the ratio of the coating to substrate thickness. Hence one equation which could be used to determine the residual stress of a thin deposit often is unsuitable for that of thick deposits. This paper describes the equations used in the literature to predict residual stress and both quenching and cooling stresses. These analytical equations are applied to experimental data and compared to the FEA models (Ref 4) and experimental residual stress results (Ref 2).

2. Residual Stress Determination

In the current study, WC-Co was deposited using the Sulzer Metco DJ HVOF process onto 30 strips (generally 20 mm wide × 80 mm long) of AISI 316L stainless steel, according to Table 1 (Ref 1, 2), where coating thickness (0.2-3 mm) and substrate thickness (0.075-2 mm thick) were varied. The Young's modulus values used in the residual stress equations, for the coating and the substrate were 185 GPa (found as part of the present study using a cantilever test, Ref 15) and 200 GPa (Ref 16), respectively.

Table 1 Spraying parameters for WC-Co material (Ref 1, 2)

Parameters	Diamalloy 2003 WC-Co		
Gases:	Oxygen	Propylene	Air
Pressure, bar, psi	10.4 (150)	6.9 (100)	5.2 (75)
Flow, SLPM	265.4	73.1	325
Spray rate, g/min (lb/h)	38 (5)		
Spraying distance, mm (inches)	200 (8)		

SLPM, standard liters per minute

2.1 Analytical Methods for Predicting Residual Stresses

Residual stress may be calculated analytically using the curvature (by measuring the resulting deflection of the sample) and the physical properties of the sample. Various equations exist and they can be classified according to the prediction of quenching and cooling and the final residual stress of a deposit. The research paper looks at the most popular equations used.

2.1.1 Quenching Stresses. The quenching stress (deposition stress) caused on impact and quenching of individual lamella, has been shown to be (Ref 17, 18):

$$\sigma_q \approx \alpha_c(T_m - T_s)E_c \quad \text{(Eq 1)}$$

where α_c, T_m, T_s, E_c, are the deposit coefficient of thermal expansion, lamella melting and substrate temperatures, and deposit apparent Young's modulus values, respectively. Another equation often used is (Ref 19):

$$\sigma_q = \frac{[E_c(T_m - T_s)(\alpha_c)]}{[1 - \nu_c]} \quad \text{(Eq 2)}$$

This equation is similar to Eq 1, except the effective coating Young's modulus E'_c is used:

$$E'_c = \frac{E_c}{(1 - \nu_c)} \quad \text{(Eq 3)}$$

where ν_c represents the coatings Poisson's ratio.

2.1.2 Cooling Stresses. The cooling stress (postdeposition stress) caused due to thermal mismatch between the substrate and deposit post spraying can be estimated by the following (Ref 20, 21):

$$\sigma_{cooling} = \frac{[E_c(T_s - T_R)(\alpha_c - \alpha_s)]}{\left[1 + 2\left(\frac{E_c t_c}{E_s t_s}\right)\right]} \quad \text{(Eq 4)}$$

where E_s is the substrate stiffness, α_s, T_R, t_s, and t_c are the substrate coefficient of thermal expansion, room temperature, and the thicknesses of the substrate/deposit, respectively.

2.1.3 Residual Stress. The final overall stress at the coating surface can be obtained by adding the quenching stress result to the cooling stress result. Whether the cooling stress in the coating is tensile or compressive depends upon the relative values of these expansion coefficients. If, as the temperature decreases, the coating contracts to a greater extent than the substrate ($\alpha_c > \alpha_s$), a tensile stress is generated in the coating. This may lead to adhesion loss and cracking of the coating or formed material (Ref 22). If the coefficients are equal, no cooling stress will develop. However, if the coating contracts by a smaller amount than the substrate ($\alpha_c < \alpha_s$), the resulting cooling stress will be compressive (Ref 18).

A number of equations have been derived to determine both overall coating residual stress and stress distribution through the sample. The Stoney equation (Ref 23) is a natural start, where:

$$\sigma_{RS} = \frac{[E_s \cdot t_s^2]\kappa}{[6t_c]} \quad \text{(Eq 5)}$$

This Stoney equation was modified to take into account the effective substrate Young's modulus E'_s:

$$E'_s = \frac{E_s}{(1-\nu_s)} \quad \text{(Eq 6)}$$

to form the equation:

$$\sigma_{RS} = \frac{[E_s \cdot t_s^2]\kappa}{[6(1-\nu_s)t_c]} \quad \text{(Eq 7)}$$

where κ and ν_c represents the coatings curvature and Poisson's ratio, respectively. A general expression was obtained by Clyne (1996) (Ref 22) for the curvature arising from the imposition of a uniform misfit strain, $\Delta\varepsilon$, such as would arise during a change in temperature ($\Delta\varepsilon = \Delta\alpha \cdot \Delta T$). Therefore the analytical curvature of a thermally sprayed sample can be related by the following equation:

$$\kappa = \frac{6E_cE_s(t_c+t_s)t_ct_s\Delta\varepsilon}{E_c^2t_c^4 + 4E_cE_st_c^3t_s + 6E_cE_st_c^2t_s^2 + 4E_cE_st_ct_s^3 + E_s^2t_s^4} \quad \text{(Eq 8)}$$

Shaw (Ref 17) derived an equation to predict residual stress as follows:

$$\sigma_{RS} = (\alpha_s - \alpha_c)(T_m - T_s)\frac{E_c(1-\nu_c)}{(1-\nu_c)^2} \quad \text{(Eq 9)}$$

While Senderoff and Brenner's equation for residual stress has a more complicated form (Ref 20, 24):

$$\sigma_{RS} = \frac{E_s}{(1-\nu_s)} \cdot \left[\frac{\left(t_s + \frac{E_c(1-\nu_s)}{E_s(1-\nu_c)}t_c\right)^3}{6t_st_c\left(\frac{1}{\kappa}\right)} \right] \quad \text{(Eq 10)}$$

Clyne et al. (Ref 22, 25-27) used an analytical method which considers a pair of plates bonded together with a misfit strain $\Delta\varepsilon$ in the x-direction. Distributed residual stress results are derived for the top of the deposit, each side of the deposit/substrate interface and the bottom surface of the substrate, as follows:

$$\sigma_{coating}\big|_{y=t_c} = -\Delta\varepsilon\left(\frac{E'_cE'_st_s}{t_cE'_c + t_sE'_s}\right) + E'_c\kappa(t_c - \delta) \quad \text{(Eq 11)}$$

$$\sigma_{coating}\big|_{y=0} = -\Delta\varepsilon\left(\frac{E'_cE'_st_s}{t_cE'_c + t_sE'_s}\right) - E'_c\kappa\delta \quad \text{(Eq 12)}$$

$$\sigma_{substrate}\big|_{y=0} = -\Delta\varepsilon\left(\frac{E'_cE'_st_s}{t_cE'_c + t_sE'_s}\right) - E'_s\kappa\delta \quad \text{(Eq 13)}$$

$$\sigma_{substrate}\big|_{y=-t_s} = \Delta\varepsilon\left(\frac{E'_cE'_st_s}{t_cE'_c + t_sE'_s}\right) - E'_s\kappa(t_s + \delta) \quad \text{(Eq 14)}$$

where δ is the shift of neutral axis and $\Delta\varepsilon$ is the misfit strain given by:

$$\Delta\varepsilon = (\alpha_s - \alpha_c)(T_m - T_R) \quad \text{(Eq 15)}$$

2.2 Comparative FEA Modeling

In this research, an ANSYS finite element program was used to predict the residual stress in the coated sample. A substrate material (stainless steel) is coated with WC-Co to a certain thickness. During deposition, stresses (quenching of lamella and cooling of coating) generate, generating a moment at the ends of the sample, causing the sample to deflect. The simulation of both the quenching and cooling stresses in one system is quite difficult hence the method of simulation used in the present study relied on the deformation of the final sample postspraying. To demonstrate the numerical formulation for this system, two simple approximation methods were analysed.

Hence two-dimensional modeling of the residual stress was carried out in two ways; one to model the quenching stresses as droplets and in turn layers were applied to predict the stresses during deposition. This was based on the modeling technique where various temperatures were applied to a coated sample of known thickness and then measure the stress through the tungsten carbide-cobalt deposit when the resulting deflection measured in the FEA, equaled that found experimentally in the Clyne's method. In this case, the applied temperature in the finite element system generated a thermal load in the center of the beam, and caused the beam to deflect (Fig. 1), similar to that used by Steffens et al. (Ref 8).

Similarly this system was also simulated (second method) by applying a known deflection (measured experimentally) to the sample and compared to the latter. The system was simulated by locking both ends of the sample while subjecting the center of the sample to a 'thermal load' (to generate the deflection) by applying various loads horizontally to the deposit in a tensile manner and similar loads to the substrate in a compressive manner, to generate a moment until a deflection the same as that found experimentally was attained. The choice of tensile or compressive applied to either the deposit/substrate depended on the stress that existed in the experimental sample. The basis of this technique may be found in Ref 4. The load and in turn deflection creates an

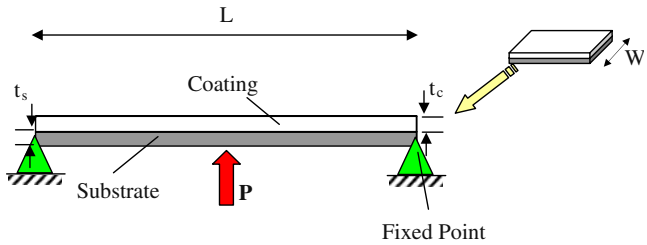

Fig. 1 Coated sample subjected to a central displacement

internal stress in the deposit causing permanent bending in the sample. In each case, the coating was considered as a homogeneous field; however, the dimensions used in the models matched that of the samples produced experimentally. For each model, a coupled field PLANE13 element was used which has 2D thermal and structural field capability. It is defined by four nodes with up to four degrees of freedom per node and has large deflection and stress stiffening capabilities and in some cases large strain capabilities.

2.2.1 Comparative Method. To validate the results found from the analytical method, the experimental results of ten of these samples ranging from a deposit surface compressive stress of 26 MPa to a tensile stress of 82 MPa were selected. Five of these coated samples were polished (plane ground using a P60 SiC abradable grit, working down to a 0.02 μm Nap Cloth) and the residual stress was measured using the Siemens 500 X-ray diffraction system, supported by the Bruker AXS Diffrac software with a diffraction scanning range from −110° to +165° for 2θ. The residual stress was measured for the final five-coated samples using the Vishay Measurements Group RS-200 Milling Guide (hole-drilling technique) (Ref 2, 4) were also measured. The strain gauge rosettes used in the study were the Vishay CEA-06-062UM-120 precision strain gauges, which are constructed of self-temperature-compensated foil on a flexible polymide carrier and incorporate a centering target for use with a precision milling guide as described in ASTM E1561. The test is carried out by connecting the strain gauge to a strain-gauge instrument (strain-recording instrument) P-3500. The hole is drilled through the coating/deposit via the central region of the strain gauge to relax the residual stress in the material being measured. Residual stress of the samples using these two techniques were then compared to Clyne's analytical method and in turn used to validate the models.

3. Results and Discussion

A series of coating conditions were used with the equations described. This mainly involved the scenario from $t_c \gg t_s$ to $t_c \ll t_s$. The objective of this research is to identify the equations best used for thick deposits. Table 2 describes the mechanical properties used and Table 3 describes the results observed.

3.1 Comparison of Quenching Stress Results

Equation 1 estimates a quenching stress of 3.40 GPa for all scenarios as this equation does not take into account the effect of varying coating or substrate thickness. Equation 2 although includes the effective coating

Table 2 Mechanical properties used in the study

Mechanical property	Unit
α_c, Coefficient of thermal expansion of the coating	8.0×10^{-6}/K
α_s, Coefficient of thermal expansion of the substrate	16.0×10^{-6}/K
T_m, Lamella melting temperature	3070 K
T_s, Substrate temperature	775 K
T_R, Room temperature	293 K
E_c, Coating Young's modulus	183.6 GPa
E_s, Substrate Young's modulus	200 GPa
ν_c, Coatings Poisson's ratio (−)	0.26
ν_s, Substrate Poisson's ratio (−)	0.3

Table 3 The effect of stress on various coating/substrate thickness analytically and using the finite element technique

	Sample thickness					
Stress equation used	**t_c = 0.2 mm t_s = 0.075 mm**	**Thickness ratio t_c/t_s = 2.67**	**t_c = 1 mm t_s = 0.075 mm**	**Thickness ratio t_c/t_s = 13.33**	**t_c = 0.2 mm t_s = 1 mm**	**Thickness ratio t_c/t_s = 0.2**
1. Quenching stress (Ref 17, 18)	3.40 GPa		3.40 GPa		3.40 GPa	
2. Kuroda et al., Quenching stress (Ref 19)	4.73 GPa		4.73 GPa		4.73 GPa	
3. Senderoff et al., Cooling stress (Ref 20, 21)	−0.118 GPa		−0.027 GPa		−0.513 GPa	
4. Pawlowski, Residual stress (1. + 3.) (Ref 18)	3.28 GPa		3.37 GPa		2.89 GPa	
5. Pawlowski, Residual stress (2. + 3.) (Ref 18)	4.61 GPa		4.70 GPa		4.22 GPa	
6. Stoney equation (Ref 23)	92.0 MPa		1.60 MPa		26.7 GPa	
7. Modified Stoney equation (Ref 23)	0.13 GPa		2.28 MPa		3.81 GPa	
8. Shaw, Residual stress equation (Ref 17)	8.40 GPa		8.40 GPa		8.40 GPa	
9. Senderoff and Brenner, Residual stress equation (Ref 20, 24)	5.16 GPa		5.00 GPa		6.26 GPa	
10. Clyne et al., distributed residual stress (Ref 22, 25-27)						
Top of deposit	−0.17 GPa		1.75 GPa		−4.02 GPa	
Interface	−5.21 GPa		−0.44 GPa		−4.84 GPa	
Average residual stress	−2.69 GPa		−0.66 GPa		−4.43 GPa	
11. Derived quenching stress, Eq 22	2.86 GPa		0.69 GPa		5.15 GPa	
12. Model coating quenching stress	3.27 GPa		1.22 GPa		4.57 GPa	
13. XRD method surface stress	0.84 GPa		0.76 GPa		0.88 GPa	
14. Hole drilling method surface stress	0.79 GPa		0.68 GPa		0.82 GPa	

Young's modulus E'_c, it too assumes the quenching stresses to be constant for all thicknesses at 4.73 GPa. Therefore, these equations do not adequately determine these stress situations and Kuroda et al. (Ref 19) states that this equation is not suitable unless the substrate is much greater than the coating thickness ($t_c \ll t_s$). However, these equations do not take account the effect of varying coating or substrate thickness.

3.1.1 Comparison of Cooling Stress Results. Equation 4 estimates the cooling stress for all scenarios as it does take into account the effect of varying coating or substrate thickness. It provides a compressive stress result based on the thickness, Young's modulus, coefficients of thermal expansion and change in temperature during cooling. However, this equation does not take into account the effective substrate and coating Young's modulus E'_s and E'_c which is applicable to substrate/coating systems having an equal biaxial stress state (Ref 26).

3.1.2 Comparison of Residual Stress Results. First, combining the results of Eq 1 and 4 (and Eq 2 and 4, respectively) provides an overall calculation for residual stress (Ref 18). However as the quenching stresses provide poor approximations for varying thicknesses, these results are of little importance here.

The Stoney equation (Ref 23) (Eq 5) provides a varying residual stress result for each scenario taking into account all parameters such as; thickness, Young's modulus, coefficients of thermal expansion, and change in temperature during cooling and combining together with Eq 8 misfit strain effects. Equation 7, a modified version of the Stoney equation, although includes the effective substrate Young's modulus E'_s, it does not take into account the effective coating Young's modulus E'_c. Second this equation is accurate if t_c tends toward zero and κ must also tend toward zero. Thus this is unsuitable for $t_c = t_s$ and $t_c \gg t_s$ situations.

Shaw's (Ref 17) equation (9) does not take into account the effect of varying coating or substrate thickness, hence is too general for thermal spray analysis. Senderoff and Brenner's equation (10, Senderoff's formula) seems to provide a satisfactory solution for residual stress; however, Eq 8 does help this solution as it accounts for misfit strain effects. This formula can be used in the case of large deflections (indirectly proportional to κ) and are based on the elastic beam theory. However, this theory is only applicable if the width-to-length ratio of the substrate is small, hence the validity of Senderoff s formula is highly dependent on the substrate/sample geometry used.

Previous research has already described the confidence of using Clyne's equations as a measure of distributed residual stress across a deposit, when this technique was compared to X-ray diffraction and hole drilling experimental techniques (Ref 2, 4). While there were differences in the three measurement methods, correlation between the methods was reasonable, particularly for higher deposit thicknesses. These equations work for both thick and thin deposits, hence provide researchers with solutions for sample residual stress determination.

However if one was to determine the quenching and cooling stresses based on the above group of equations, it would seem that Clyne's equations (11 and 12) combined residual stress equations could be used with a form of Eq 4 (cooling stress) to determine the quenching stress result:

$$\text{Quenching stress} = \text{Residual stress} - \text{Cooling stress} \quad \text{(Eq 16)}$$

For Clyne's equations to be used a mean coating result would have to be used:

$$\left\{-\Delta\varepsilon\left(\frac{E'_c t_s E'_s}{t_c E'_c + t_s E'_s}\right) + E'_c\kappa(t_c - \delta) - \Delta\varepsilon\left(\frac{E'_c t_s E'_s}{t_c E'_c + t_s E'_s}\right) - E'_c\kappa\delta\right\}\Big/2 \quad \text{(Eq 17)}$$

Thus Eq 17 reduces to:

$$-\Delta\varepsilon\left(\frac{E'_c t_s E'_s}{t_c E'_c + t_s E'_s}\right) + \frac{E'_c\kappa \cdot t_c}{2} \quad \text{(Eq 18)}$$

If Eq 4 was modified to take into account the effective substrate and coating Young's modulus E'_s and E'_c for an isotropic in-plane stress state, there is effectively another stress equal to the x directional stress state in the z direction, thus inducing a Poisson strain in the x direction, therefore Eq 3 and 6 should be included (Ref 26), hence:

$$\sigma_{\text{cooling}} = \frac{\left[E'_c \Delta T \Delta\alpha\right]}{(1-\nu_c)\left[1 + 2\left(\frac{(1-\nu_s)E_c t_c}{(1-\nu_c)E_s t_s}\right)\right]} \quad \text{(Eq 19)}$$

which reduces to:

$$\sigma_{\text{cooling}} = \frac{\left[E'_c(T_s - T_R)(\alpha_c - \alpha_s)\right]}{\left[(1-\nu_c) + 2\left(\frac{(1-\nu_s)E_c t_c}{E_s t_s}\right)\right]} \quad \text{(Eq 20)}$$

This provides a quenching stress formula of the form:

$$\sigma_{\text{quenching}} = -\Delta\varepsilon\left(\frac{E'_c t_s E'_s}{t_c E'_c + t_s E'_s}\right) + \frac{E'_c\kappa \cdot t_c}{2} - \frac{\left[E'_c(T_s - T_R)(\alpha_c - \alpha_s)\right]}{\left[(1-\nu_c) + 2\left(\frac{(1-\nu_s)E_c t_c}{E_s t_s}\right)\right]} \quad \text{(Eq 21)}$$

which includes misfit strain, effective stiffnesses (Poisson's effect), and thickness for both the coating and substrate, coefficients of expansion and process temperatures.

However, this equation can result in either a compressive or tensile stress value, therefore if one is to achieve the tensile result for quenching stress, then the equation needs to be modified to:

$$\sigma_{\text{quenching}} = \pm\left\{-\Delta\varepsilon\left(\frac{E'_c t_s E'_s}{t_c E'_c + t_s E'_s}\right) + \frac{E'_c\kappa \cdot t_c}{2}\right\} - \frac{\left[E'_c(T_s - T_R)(\alpha_c - \alpha_s)\right]}{\left[(1-\nu_c) + 2\left(\frac{(1-\nu_s)E_c t_c}{E_s t_s}\right)\right]} \quad \text{(Eq 22)}$$

where + is used where the residual stress mean is tensile and − is used where the residual stress mean is compressive.

3.1.3 Finite Element Model. A model was designed to mimic quenching stresses and these results were compared to the quenching result found using Eq 22, Fig. 2. The model predicted a quenching stress of 6.35 GPa compared to 6.63 GPa obtained by the new analytical equation. Similar layered models (Fig. 3) were produced and compared with Eq 22, Table 3. Hence the profile of the results does appear to support each other, where the model slightly over estimates the quenching stress found. Residual stress of samples used in this study was also measured using two other techniques; XRD and the hole drilling method. Table 3 shows the results for each method. While there are differences in the four measurement methods, correlation between the methods is reasonable, as the XRD and hole drilling values are those associated to that of the coating stress state rather than intrinsic stresses. The XRD method indicates, in most cases, marginally higher stress results than the hole drilling method (this finding supports results observed by Tan, Ref 28). In the case of deposits 1 mm or greater, the XRD

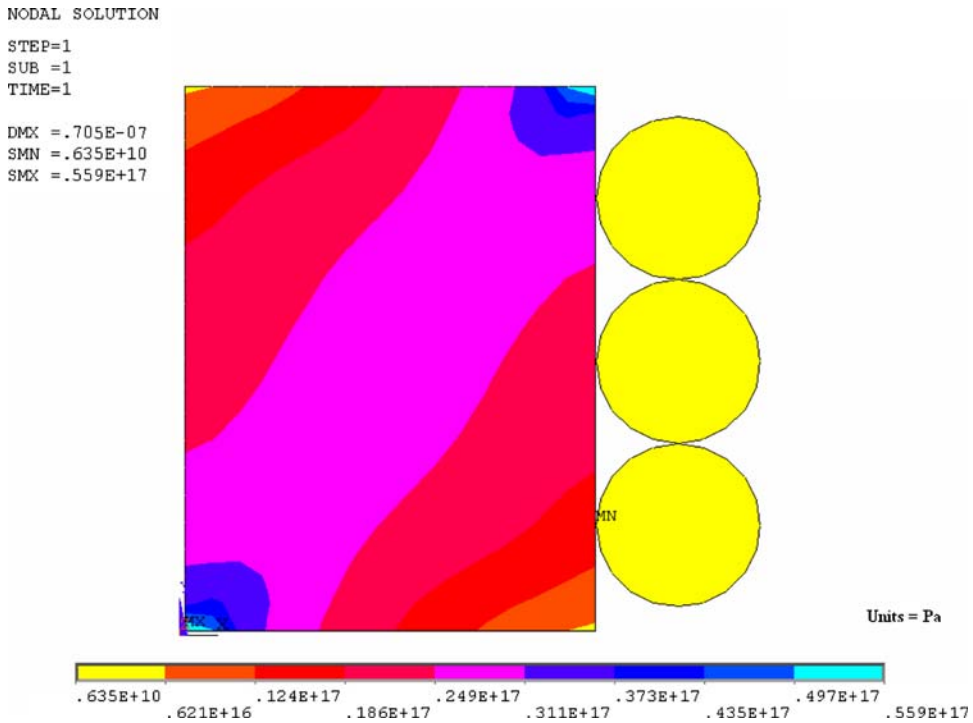

Fig. 2 Resultant *x*-directional stress results for single pass of WC-Co deposit on a 0.075-mm substrate

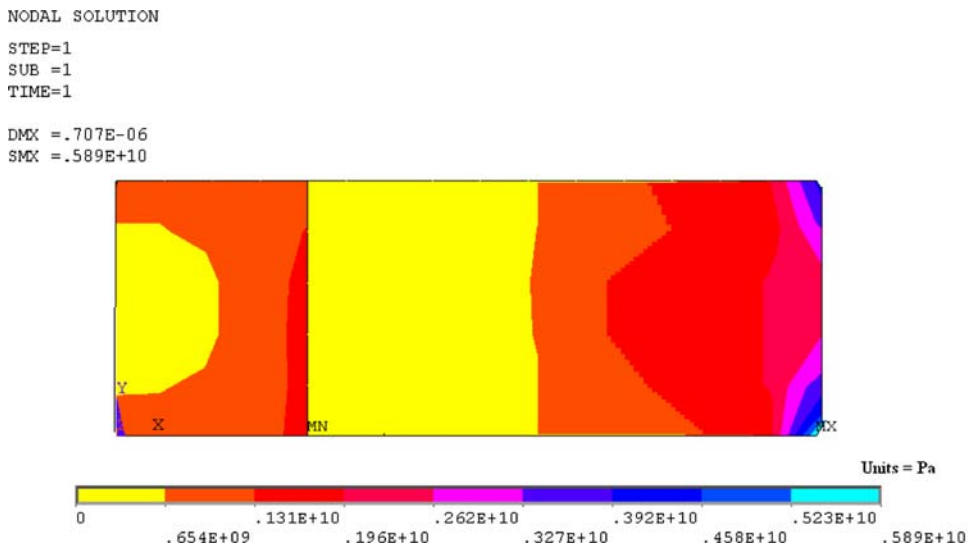

Fig. 3 Resultant x-directional stress results for 0.2 mm WC-Co deposit on a 0.075-mm substrate

results also correlate well with those found using Clyne's method. Previous research carried out by the author showed that Clyne's analytical method produced stress values approximately 30% of that found using the hole drilling and XRD methods, respectively (Ref 4).

4. Summary and Conclusion

In this study, the analysis of residual stress generated in high velocity oxy-fuel thermal spray tungsten carbide-cobalt deposits was analysed, both analytically and with the use of numerical modeling. Hence this technique was used as a benchmark in validating the results of the FE model and in turn the analytical results. The paper reviews equations previously used by various authors to predict quenching, cooling, and residual stress. The research identifies the issues with some of these equations, such as not accounting for various combinations of coating/substrate thicknesses and for the Poisson's effect, and selects two sets of equations which provide reasonable predictions of stress. An equation for the calculation of quenching stresses is deduced for both thick and thin deposits and its results are compared to models previously benchmarked against experimental data.

Although this equation may not provide an exact solution for quenching stresses, it does allow the researcher to interchange various thicknesses of coating and substrate types thus to predict the stresses produced during deposition. This enables the researcher to monitor and control the final thickness of the deposit in situations where coating thickness is desired.

References

1. J. Stokes and L. Looney, HVOF System Definition to Maximise the Thickness of Formed Components, *Surf. Coat. Tech.*, 2001, **148**(1), p 18-24
2. J. Stokes and L. Looney, Residual Stress in HVOF Thermally Sprayed Thick Deposits, *Surf. Coat. Tech.*, 2004, **177-178**, p 18-23
3. J. Stokes and L. Looney, Properties of WC-Co Components Produced Using the HVOF Thermal Spray Process, *Thermal Spray: Surface Engineering Via Applied Research*, C.C. Berndt, Ed., 8-11 May 2000 (Montréal, Québec, Canada), ASM International, 2000, p 263-271
4. J. Stokes and L. Looney, Finite Element Analysis of Residual Stress Generated by the HVOF Process, *Building on 100 Years of Success, Proceedings of the 2006 International Thermal Spray Conference*, B.R. Marple, M.H. Hyland, Y.C. Lau, R.S. Lima, and J. Voyer, Eds., May 15-18, 2006 (Seattle, WA, USA), ASM International, 2006, ISBN: 978-0-87170-836-6
5. J. Stokes and L. Looney, HVOF System Definition to Maximise the Thickness of Formed Components, *International Conference on Advances in Materials and Processing Technology*, M.S.J. Hashmi, Ed., 3-6 Aug 1999 (Dublin, Ireland), 1999, p 775-784
6. K.A. Khor and Y.W. Gu, Effects of Residual Stress on the Performance of Plasma Sprayed Functionally Graded ZrO_2/NiCoCrAlY Coatings, *Mater Sci Eng*, 2000, **A277**, p 64-76
7. X.C. Zhang, B.S. Xu, H.D. Wang, and Y.X. Xu, Modelling of the Residual Stresses in Plasma-Spraying Functionally Graded ZrO_2/NiCoCrAlY Coatings using Finite Element Method, *Mater. Design*, 2005, **27**(4), p 308-315
8. H.D. Steffens and M. Gramlich, FEM-Analysis of Plasma Sprayed Thermal Barrier Coatings, *Thermal Spray: International Advances in Coatings Technology*, C.C. Berndt, Ed., May 25-June 5, 1992 (Orlando, FL), ASM International, 1992, p 531-536
9. J.K. Wright, J.R. Fincke, R.N. Wright, W.D. Swank, D.C. Haggard, Experimental and Finite Element Investigation of Residual Stress Resulting from the Thermal Spray Process, *Advances in Thermal Spray Science & Technology*, C.C. Berndt and S. Sampath, Ed., Sept 11-15, 1995 (Houston, TX), ASM International, 1995, p 187-192
10. H. Gruhn, W. Fischer, C. Funke, W. Mallener, and D. Stover, Residual Stress Calculation by Finite Element Methods, *Thermal Spray: Practical Solutions for Engineering Problems*, C.C. Berndt, Ed., Oct 7-11, 1996 (Cincinnati, OH), ASM International, 1996, p 869-874
11. H. Gruhn, W. Malliner, and D. Stover, Modeling of Residual Stresses in Plasma Sprayed Multilayer Systems, *Advances in Thermal Spray Science and Technology*, C.C. Berndt and S. Sampath, Ed., Sept 11-15, 1995 (Houston, TX), ASM International, 1995, p 231-236
12. C.H. Hsueh and A.G. Evans, Residuals Stresses in Metal/Ceramic Bonded Strips, *J. Am. Ceram. Soc.*, 1985, **68**, p 241-248
13. S. Suresh, A.E. Giannkopoulos, and M. Olsson, Elastoplastic Analysis of Thermal Cycling: Layered Materials with Sharp Interfaces, *J. Mech. Phys. Solids*, 1994, **42**, p 979-1018
14. B.S. Yilbas and A.F.M. Arif, Residual Stress Analysis for HVOF Diamalloy 1005 Coating on Ti-6Al-4V alloy, *Surf. Coat. Tech.*, 2007, **202**(3), p 559-568
15. E.F. Rybicki, J.R. Shadley, Y. Xiong, and D.J. Greving, A Cantilever Beam Method for Evaluation of Young's Modulus and Poisson's Ratio of Thermal Spray Coatings, *J. Therm. Spray Tech.*, 1995, **4**(4), p 377-383
16. R.E. Whan, *ASM Handbook Material Characterization*, 9th Ed., Vol. 10, G.M. Crankovic, Ed., (Metals Park, OH), American Society for Metals, 1992. ISBN: 978-0-87170-016-2
17. L.L. Shaw, Thermal Residual Stresses in Plates and Coatings Composed of Multi-layered and Functionally Graded Materials, *Compos. B Eng.*, 1998, **29**(3), p 199-210
18. L. Pawlowski, *The Science and Engineering of Thermal Spray Coatings*, John Wiley and Sons, Inc., London UK, 1995
19. S. Kuroda and T.W. Clyne, The Quenching Stress in Thermally Sprayed Coatings, *Thin Solid Films*, 1991, **200**, p 273-284
20. S. Senderoff and A. Brenner, Calculation of Stress in Electrodeposits from the Curvature of a Plated Strip, *J. Res. Nat. Bur. Stand.*, 1949, **42**(2), p 105-123
21. A.A. Tipton, The Effect of HVOF Sprayed Coatings on the Elevated Temperature High Cycle Fatigue Behaviour of a Martensitic Stainless Steel, *Proceedings of the 8th National Thermal Spray Conference*, C.C. Berndt and S. Sampath, Eds., 1995 (Houston, Texas), 1995, p 463-468
22. A. Itoh and T.W. Clyne, Initiation and Propagation of Interfacial Cracks During Spontaneous Debonding of Thermally sprayed coatings, *Proceedings of the 8th National Thermal Spray Conference*, C.C. Berndt and S. Sampath, Eds., 1995 (Texas, USA), 1995, p 425-432
23. G.G. Stoney, The Tension of Metallic Films Deposited by Electrolysis, *Proc. Roy. Soc.*, 1909, **A82**, p 172-175
24. R.O.E. Vijgen and J.H. Dautzenberg, Mechanical Measurement of the Residual Stress in thin PVD Films, *Thin Solid Films*, 1995, **270**, p 264-269
25. T.W. Clyne and S.C. Gill, Residual Stresses in Surface Coatings and Their Effects on Interfacial Debonding: A Review of Recent Work, *J. Therm. Spray Tech.*, 1996, **5**(4), p 401-418
26. Y.C. Tsui and T.W. Clyne, An Analytical Model for Predicting Residual Stresses in Progressively Deposited Coatings, Part 1: Planar Geometry, *J. Thin Solid Films*, 1997, **306**, p 23-33
27. T.W. Clyne, Residual Stresses in Surface Coatings and Their Effects on Interfacial Debonding, *Key Eng. Mats.*, 1996, **116-117**, p 307-330
28. J.C. Tan, L. Looney and M.S.J. Hashmi, Residual Stress Analysis of WC-Co Solid Components Formed by the HVOF Thermal Spraying Process, *Adv. Powder Metall. Partic. Mater.*, 1996, **3**, p 9.41-9.52